Mechanical response of shells to tube rupture in shell-and-tube heat exchangers

Colin Deddis, Director, Greymore Engineering Services Ltd, Slioch Orchard Grove, Echt, Westhill, AB32 6UL

Rob Kulka, Section Manager, Asset Integrity Management, TWI Ltd, Granta Park, Great Abington, CB21 6AL

Alan Clayton, Director, A M Clayton Ltd, 30 Oban Grove, Fearnhead, Warrington, WA2 0TG

Mark Scanlon, Head of HSE Good Practice, Energy Institute, 61 New Cavendish Street, London W1G 7AR, UK

A frequently encountered scenario in the operation of a shell and tube heat exchanger is that of high pressure gas on the tube side and liquid flowing through the shell, whose design pressure is rated at a much lower value. In the event of a tube rupture an initial shock pulse is passed into the shell which rapidly decays with distance. As gas then flows from the broken tube into the liquid it creates an expanding bubble which forces liquid out of its path. This results in a transient pressure surge, similar to water hammer, which travels at the speed of sound in liquid. This transient pressure can be much higher than the normal operating pressure of the liquid flowing in the shell and can therefore cause an overpressure with resultant loss of containment. The Energy Institute published guidance on this phenomenon and how to design the heat exchanger and its overpressure protection systems in the second edition of "Guidelines for the safe design and operation of shell and tube heat exchangers to withstand the impact of tube failure."

Conventional static analysis is currently used for determining the shell stresses during a tube rupture despite its dynamic nature. The work presented in this paper was motivated by a concern that a tube rupture may result in shell vibration, to a level which may damage or fail the shell wall.

The work demonstrates the need to account for a dynamic magnification of the pressure imposed on the shell due to the structural response of the heat exchanger during a tube rupture.

The paper introduces a new concept for evaluating the dynamic effects on the shell without the need for extensive structural modelling. Results used to validate this approach will be presented along with a methodology which will be incorporated in the third edition of the Energy Institute guidelines in late 2021.

Adopting this methodology will ensure that heat exchangers and their overpressure protection systems are adequately designed to prevent a loss of containment in the unlikely but credible event of a tube rupture.

Keywords: Shell and tube heat exchanger, overpressure, tube rupture

Background

Many shell and tube heat exchangers are designed to exchange heat between a low pressure liquid in the shell side and a high pressure gas in the tube side. The design of the low pressure side of the heat exchanger and its overpressure protection needs to account for the possibility of tubes failing in service. A tube failure can take the form of a small leak which develops over time or, of more concern, a sudden failure, referred to as a tube rupture. In both cases the passage of high pressure gas into the low pressure liquid can potentially lead to an increase in pressure in excess of the safe design limits of the shell. This in turn can result in the shell failing with a catastrophic loss of containment in the absence of an adequately designed overpressure protection system.

Designing a heat exchanger to withstand the impact of a sudden tube failure (tube rupture) poses a particular challenge due to the rapid changes in pressure and flow within the low pressure liquid as gas expands through the broken tube. This problem has been the subject of two Joint Industry Projects (JIPs) managed by the Energy Institute and the former Institute of Petroleum. The first JIP studied the dynamics of tube rupture and published the first edition of *Guidelines for the safe design and operation of shell and tube heat exchangers to withstand the impact of tube failure.* The second JIP concentrated on the response time of overpressure protection devices and the impact of the overpressure systems design on downstream relief systems. This work was incorporated in an expanded second edition of the *Guidelines*[2], published in 2015.

The current guidance accounts for the dynamic changes in fluid properties and the dynamic response of the pressure relief devices during a tube rupture. However, it assumes that the shell stresses can be determined from a conventional static analysis in applying the fluid pressure to the shell wall. The allowable stresses specified in the pressure vessel design publications apply to static pressure loading. In reality the shell is not a static structure but will vibrate due to the rapidly changing fluid pressure. This paper summarises investigations into whether the shell vibration could be to a level which may damage or fail the shell wall and the resulting guidance on dynamic structural analysis.

Surge Caused by Tube Rupture

The mechanical response of the shell is driven by the pressure changes in the fluid. Figure 1 illustrates what happens following a tube rupture. As high pressure gas escapes through the broken ends of the tube into the liquid it forms a bubble which expands in volume due to the reduction in pressure and influx of gas. The gas bubble must overcome the inertia of the liquid in the shell as it expands. This causes a step wise increase in the local pressure which is transmitted through the liquid in all directions as a surge front at the speed of sound.

Figure 1: Schematic Representation of Tube Rupture

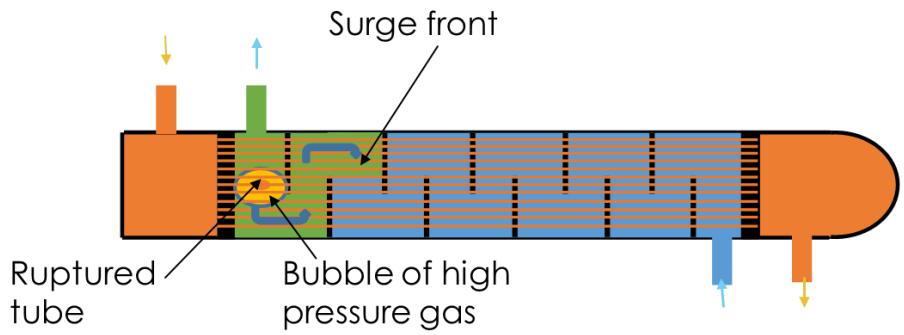

The magnitude of this initial surge pressure P_{is} is dependent on the pressure of the gas in the tubes, P_o, the initial pressure in the liquid, P_r, the fluid properties (γ, a, ρ_l, c), the coefficient of discharge for the open end of the tube, C_D, and the effective areas of the shell A_s and the tubes, A_t. It can be estimated from Equation 1.

$$P_{is}(P_{is} - P_r)^{\gamma} = \left(\frac{2}{\gamma+1}\right)^{\gamma/\gamma-1} P_0 \left(\frac{C_D a \rho_l c A_t}{A_s}\right)^{\gamma} \qquad \text{Equation 1}$$

Figure 2 represents the pressure exerted at any point along the length of the shell with time. The shock due to the release of mechanical energy when the tube breaks is very short lived (microseconds) and this is followed by the surge pressure described above. If the surge pressure wave encounters a "dead end" such as a closed valve in the liquid outlet, it is reflected and will travel back along the shell towards the point of rupture now doubled in amplitude. At some point the relief device will operate allowing the pressure to decay. All of this happens within a timescale of up to several hundred milliseconds.

Figure 2 Schematic of Pressure in Shell

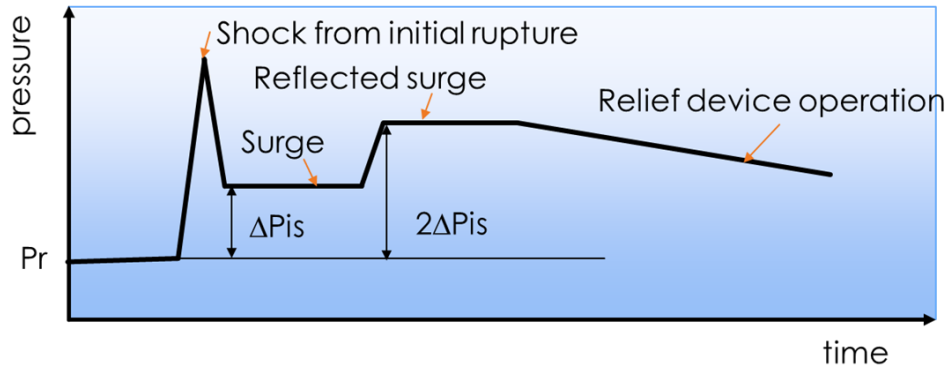

Shell Response to Tube Rupture

Analysis Approach

It was firstly important to understand whether or not the short duration, high magnitude pressure peaks (labelled 'shock from initial rupture' in Figure 2), are capable of causing failure of the low pressure side of the exchanger. The results of a study of short term loading identified that this shock will die out before reaching the shell wall, except for instances of rupture in the outer part of a tube bundle, where the stresses will not be higher than those resulting from the one dimensional step pressure, and over a very small area.

The longer pressure surge may have a significant effect on the shell response. The magnitude of this surge may double in magnitude if the surge rebounds off an internal surface before the relief device operates. Rapid loading of the shell can result in wall vibration which alters the shell stresses.

Two approaches were taken to identify and quantify these effects, one based on a single degree of freedom analysis and the other carrying out extensive finite element calculations, using the Abaqus finite element analysis solver.

Single Degree of Freedom Model

The shell of a heat exchanger can potentially have a very wide range of vibration modes and corresponding frequencies, but comparison with strain gauges on previous vessel tests carried out by the Health and Safety Laboratory (HSL) showed that only one frequency was significant, the ring breathing mode (radial vibration) frequency, which is induced as the surge passes any given section of the shell. Where a single mode is dominant its effect can be evaluated using a single degree of freedom (mass on a spring) model generating forced harmonic motion, as given by Equation 2, where Δr is the radial

displacement, Δr_s is the radial displacement for the peak pressure when treated as static loading, ω is the natural frequency of vibration, $p(t)$ is the pressure at any time (t), and p_0 is the peak pressure at the specific location.

$$\frac{d^2}{dt^2}\left(\frac{\Delta r}{\Delta r_s}\right) + \omega^2\left(\frac{\Delta r}{\Delta r_s}\right) = \frac{p(t)\omega^2}{p_0} \qquad \text{Equation 2}$$

The stresses from the surge pressure are strongly dependent on the rise time to the quasi-steady state and a worst case assumption based on the HSL tests suggests a rise time Δt of 0.6 ms.

Figure 3 Schematic of Shell Response to Tube Rupture.

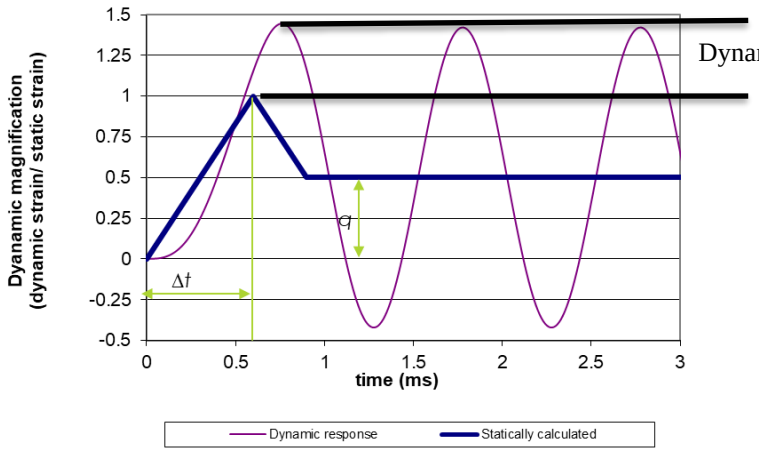

Dynamic Load Factor (DLF) =1.4

The ring breathing mode has a frequency, f_s, which is dependent on the Young's Modulus (E), Poisson's Ratio (ν), the shell material density (ρ), and the mean radius (r). It can be obtained from Equation 3.

$$f_s = \frac{1}{2\pi}\sqrt{\frac{E}{\rho(1-\nu^2)r^2}} \qquad \text{Equation 3}$$

The dynamic magnification of the shell wall stresses over applying the step pressure as a static load is given in Figure 4. The actual pressure multiplied by the dynamic load factor is defined as the effective pressure. For small STHEs (typically with large values of f_s), Figure 4 shows that dynamic effects are negligible and the effective pressure then equals the actual pressure.

Results are shown for different ratios of the initial pressure and sustained surge amplitudes (where the q ratio is the surge pressure divided by the initial pressure, where q=1 implies no reduction in pressure from the initial rise and q=0 implies no sustained surge).

The curves in Figure 4 are expressed as the maximum dynamic magnification over the peak static value. The static value is that during the pulse response if it is present or the quasi-steady state surge pressure if it is not. As can be seen, stress magnification depends on ($f_s\Delta t$) and on the surge pressure/initial pressure ratio, q.

Figure 4 Variation of dynamic load factor with frequency f_s, rise time Δt and q (sustained surge pressure to initial pressure ratio). With no reduction in surge pressure magnitude following rise, q = 1.

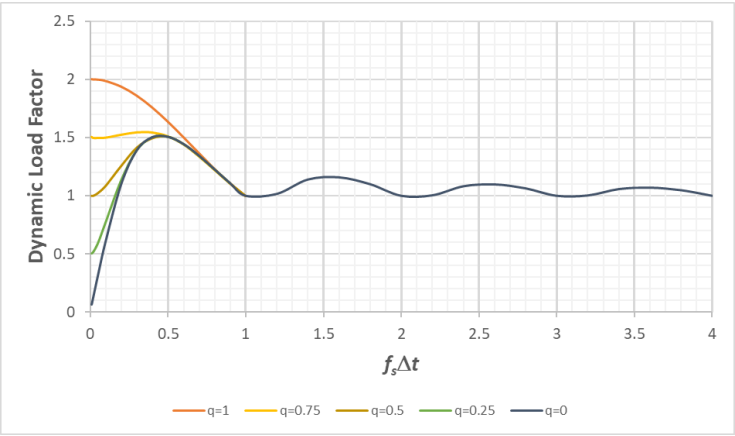

It is worth noting in Figure 4 that for initial pressure rises similar to the sustained surge pressure (q at or near unity) low frequencies give the highest dynamic magnifications, whilst for large initial pressures relative to the surge quasi-steady state

(*q* at or near zero) higher frequencies are required to give the highest dynamic magnification. This is because the natural frequency has to be high to respond to the short duration transient but lower frequencies have time to respond to the steady surge.

Finite Element Modelling Basis

Abaqus was used to analyse the stresses in three typical STHEs (a large 2-pass STHE, a medium diameter STHE, and a small diameter STHE). A model of each heat exchanger was created using shell elements. In order to achieve an accurate resolution of the stress state, the models were finely meshed.

The analysis was first validated by calculating the equivalent von Mises stress in the HSL tests and comparing this with the values deduced from the strain gauges. The pressure loading was as captured by the HSL tests at specific pressure gauge positions. The FE models were split into sections between the positions of the baffles, with the pressure transients applied to the internal surface of the cylindrical shells (and the tube sheets, head, nozzles and internal geometries where relevant). The pressure transients relevant to each baffled section were based on the flow path length position, appropriately interpolated where some baffled sections did not have working pressure gauges attached.

The comparison of calculated and measured pressures is shown in Figure 5.

Figure 5 Finite Element calculated and measured stresses near tubesheet for HSL test vessel

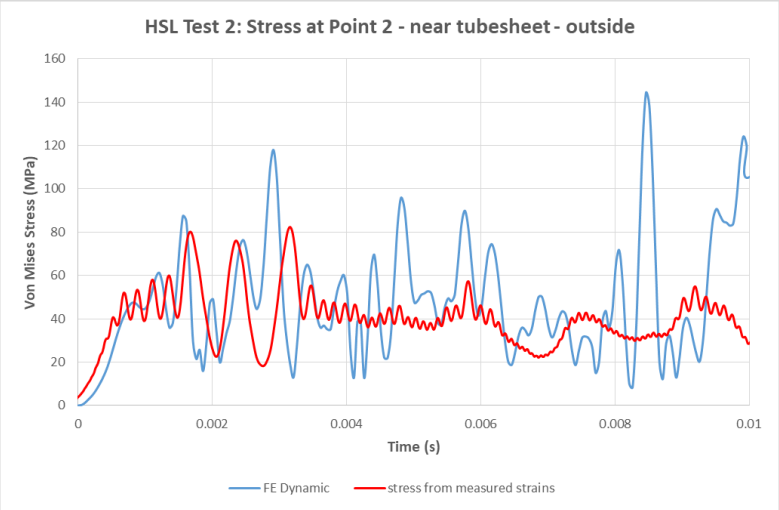

The comparison is good at short times but there is damping of the measured values at later times which gives significantly lower stresses than in the undamped finite element calculations. On this basis, allowing for damping, the finite element methods were considered suitable to evaluate the typical small, medium and large heat exchangers, shown in Figure 6.

The pressure histories at intervals along the shells were provided from the simulations reported in the Energy Institute guidelines[2] (Annex I).

Figure 6 Small, medium and Large STHE finite element models

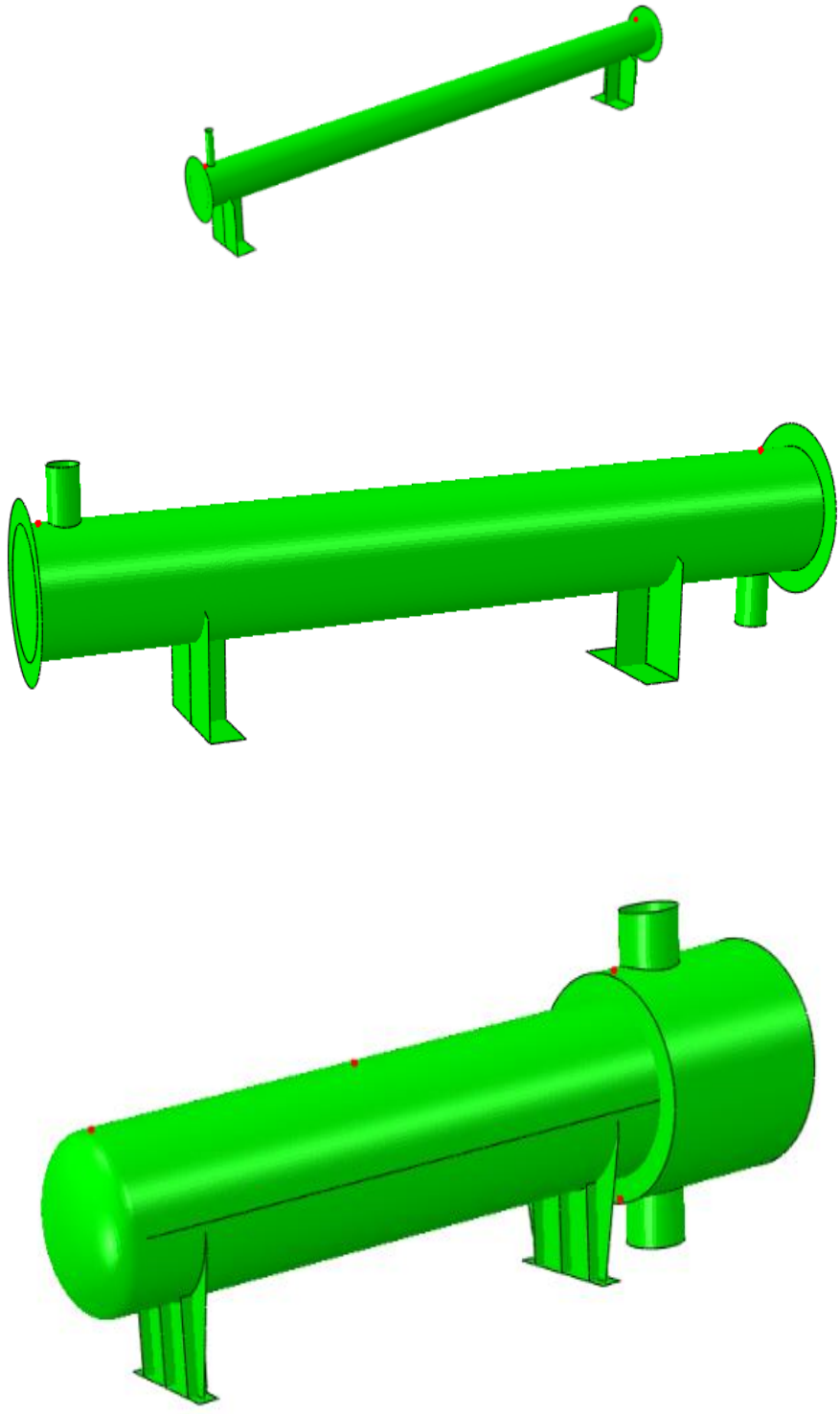

Finite Element Modelling Results

The resulting stresses from these analyses are shown in Figures 7-9.

Figure 7 Small heat exchanger: comparison between static and dynamic analysis

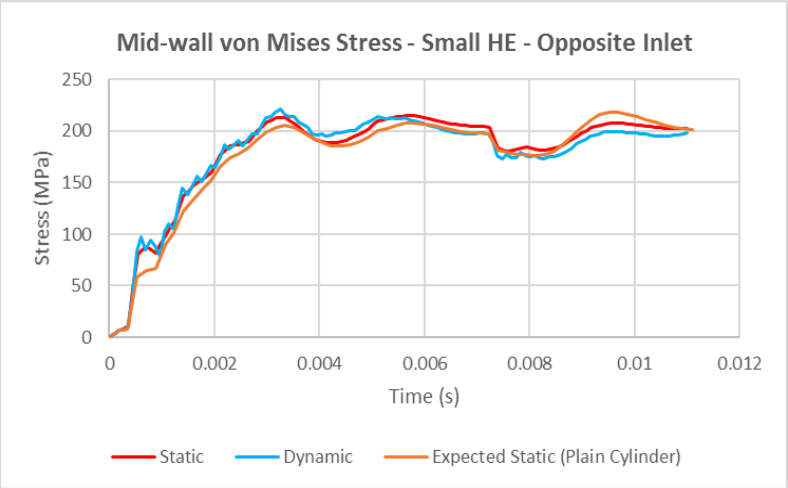

Figure 8 Medium heat exchanger: comparison between static and dynamic analysis

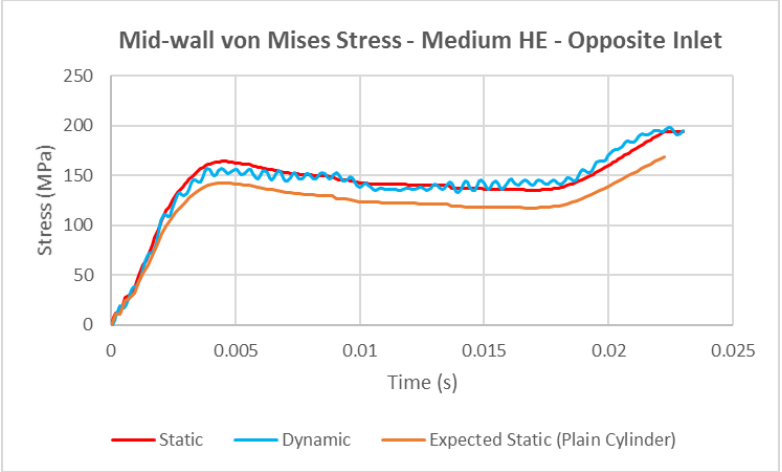

Figure 9 Large heat exchanger: comparison between static and dynamic analysis

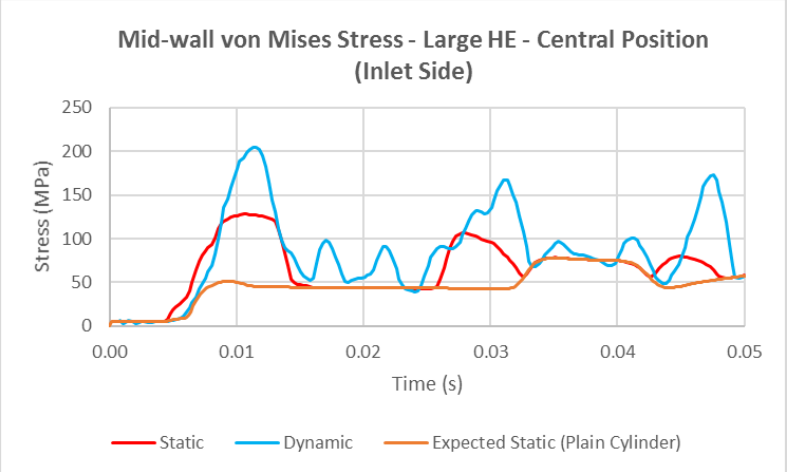

These plots display the full dynamic stress history, the static stress distribution as if the pressure history was frozen at any time and the stress if the shell were treated as a simple cylinder using the local static pressure. Any deviation between the cylinder stress and the static stress arises from stress concentrations such as nozzles, or in the case of a shell two pass heat exchanger the deviation arises from the transient differences in pressure in each pass. Deviation between the static and dynamic values is a dynamic magnification.

The graphs show little dynamic enhancement from the small and medium STHEs. This can be compared with Figure 4 predictions, replot in Figure 10, for which for the small heat exchanger would give no enhancement (dynamic load factor = 1) and the medium heat exchanger would give an enhancement of 1.02. The large heat exchanger would have a dynamic enhancement of 1.5, reasonably close to the finite element result of 1.6, even though the large heat exchanger is a two pass design. This suggests that Figure 4 gives reasonable results for dynamic enhancement and also that only large heat exchangers have significant dynamic enhancements.

Figure 10 Comparison of finite element analysis results with single degree of freedom model

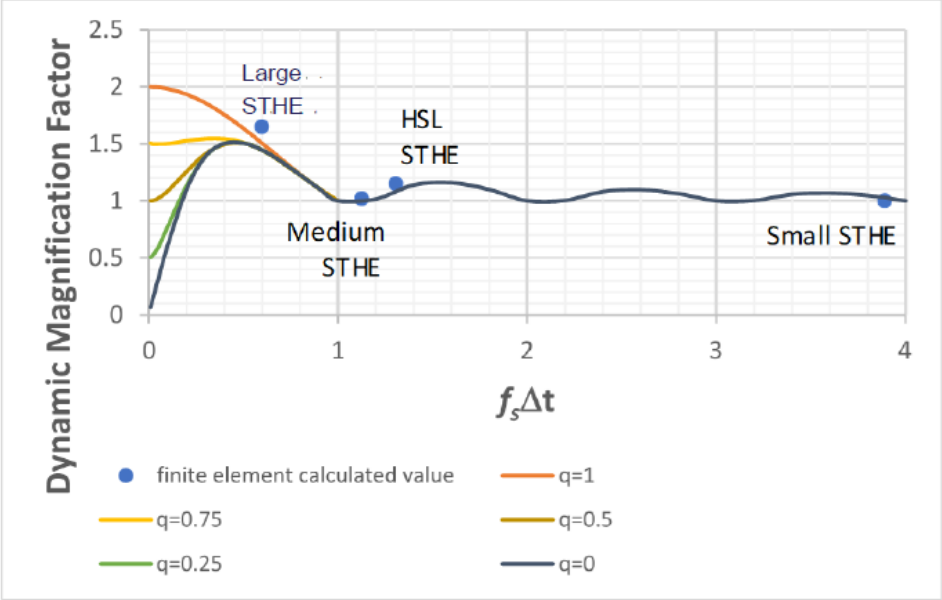

Conclusions of Mechanical Response Modelling

Based on the single degree of freedom analysis and finite element modelling, the following conclusions may be drawn:

- Statically calculated surge stresses can be approximated by simple pressurised cylinder equations.
- Dynamic enhancement to the static stress caused by the shell wall oscillating as the surge passes appears to be associated only with the cylinder ring breathing mode.
- Small and medium sized STHEs with radii in the range of approximately 100mm to 500mm have insignificant dynamic magnification of the statically determined stresses.
- For larger heat exchangers, dynamic magnification of stresses is more significant.
- The duration of dynamic oscillations is limited to a few cycles because of the damping of the fluid in the shell.
- Should the tube fail close to the shell there is the possibility of impulsive full tube pressure pulse impacting the wall which may result in high localised stresses.

Design Guidance

The current work demonstrates the need to account for a dynamic magnification of the pressure imposed on the shell due to the structural response of the heat exchanger during a tube rupture. This has implications for selecting an appropriate design pressure and relief devices for the shell.

Figure 11 Schematic showing initial impulse step pressures

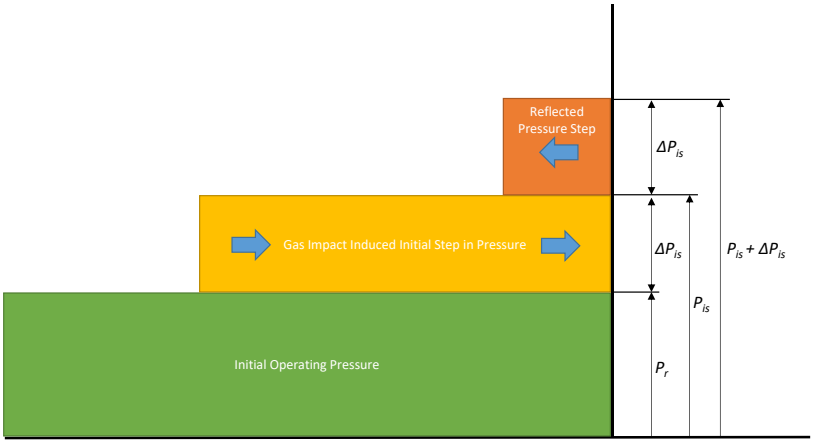

Figure 11 from the current *Guidelines* illustrates how the pressure in the shell is influenced by the tube rupture based on a static analysis. The pressure in the fluid rises local to the tube rupture and propagates outwards in both directions through the heat exchanger with an amplitude of ΔP_{is}. Where this pressure wave encounters a dead end, it is reflected adding a further ΔP_{is} to the pressure. A tube rupture could occur at any point within the tube bundle; therefore, it is unlikely that a pressure relief device will be installed in close proximity to the break in order to prevent the shell being subject to a structurally significant stress. Setting the initial design pressure of the low pressure side at or above $P_r + 2\Delta P_{is}$ protects the shell from overpressure in the time between the tube rupture occurring and the relief device responding. It also enables a choice of relief device including spring-loaded relief valves or pin valves as it accommodates the reflected pressure from the closed relief valve. Setting the pressure lower than this value means that a rupture disc is required for overpressure protection.

The current methodology can be modified to take account of the possibility of structural resonance due to the dynamic magnification by applying a dynamic load factor (DLF) to the surge pressure. This establishes an *effective pressure* which approximates the stress experienced by the shell in excess of the stress due to fluid pressure.

Figure 12 illustrates how the *effective pressure* relates to the options for setting the design pressure of the shell and the corresponding overpressure protection requirements for tube rupture. The *absolute minimum* design pressure for the shell (based on guidance in API521[1]) needs to be set such that the corrected hydrotest pressure is equivalent to the *incident pressure* imposed by the surge taking account of dynamic magnification i.e. $P_r + \Delta P_{is}.DLF$. Setting the shell side design pressure at the *peak reflected pressure* of $P_r + 2\Delta P_{is}.DLF$ enables a relief valve or rupture disc to be selected as the relief device. Between the *absolute minimum* design pressure and the *peak reflected pressure*, a rupture disc is required to ensure rapid opening of the relief path without a reflected pressure wave. Setting the shell design pressure such that its corrected hydrotest pressure equals or exceeds the HP side design pressure provides an inherently safer design which negates the need for overpressure protection for the tube rupture scenario. However, this is not common industry practice given the weight loading implications for offshore installations.

Figure 12 Schematic Integrating Design Guidance for LP Side with Mechanical Response

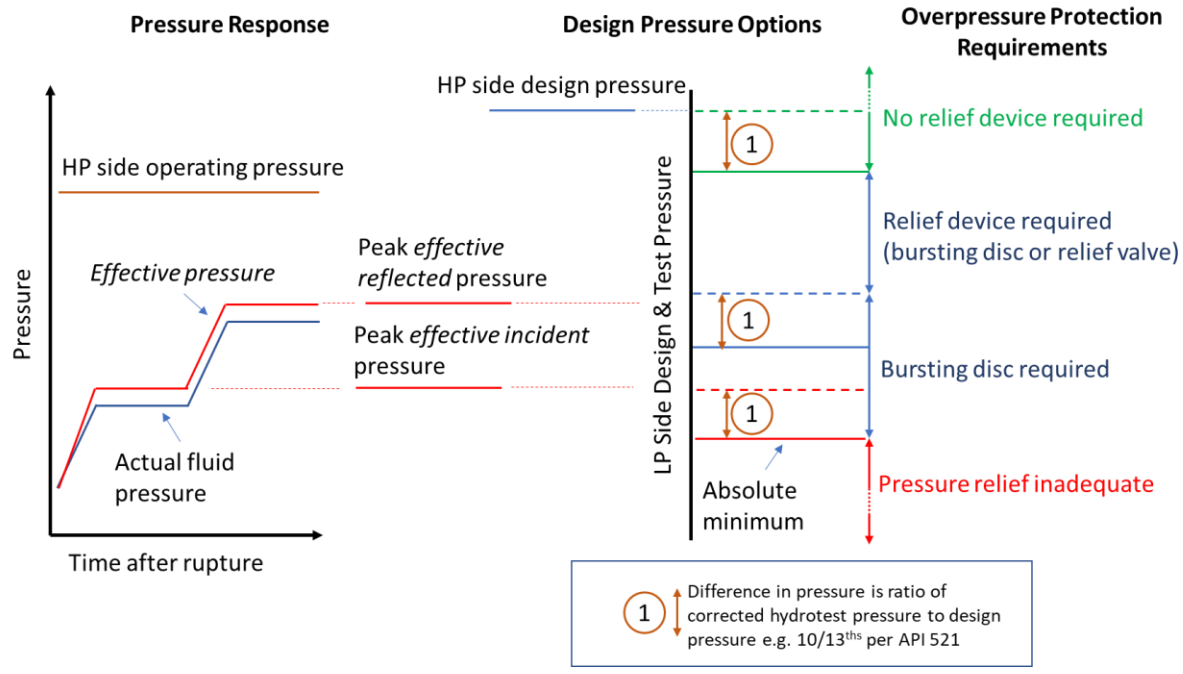

As shown by the preceding analysis the dynamic load factor (DLF) can be estimated for a shell using the single degree of freedom model which is shown in Figure 4. The most conservative basis for estimating DLF is the case when there is no reduction in surge pressure magnitude following the pressure rise, therefore, $q = 1$.

If as an example, $f_s \Delta t$ was 1.0 using a tube rupture time of 0.6 ms, the DLF from Figure 4 would be 1.0. However, if the tube took 1.9 ms to rupture, $f_s \Delta t$ would be 1.5 and DLF would be 1.2. The highest DLF should be used when assessing the structural significance of the tube rupture.

A simplified and conservative rule set which can be derived from Figure 4 is shown in Table 1 below.

Table 1 Method for Initial Estimate of Dynamic Load Factor

$f_s \Delta t_{min} < 0.8$	Use Figure 4 as DLF > 1.2
$0.8 < f_s \Delta t_{min} < 1.8$	DLF = 1.2
$1.8 < f_s \Delta t_{min}$	DLF = 1.1

Overall Conclusions

The following conclusions can be drawn from this examination of the mechanical response of low pressure liquid filled shells of heat exchangers following the rupture of a tube carrying high pressure gas:

- Under certain conditions there can be dynamic enhancement to the static stress caused by the shell wall oscillating as the pressure surge passes.
- This dynamic magnification can be estimated using a validated single degree of freedom model based on the cylinder breathing mode.
- This simplified model can be used without the need for extensive structural modelling to determine a dynamic load factor which can be applied to the fluid surge pressures following tube rupture.
- The resultant *effective pressure* imposed on the shell wall during the tube rupture event can be used to inform engineering decisions concerned with determining the design pressure of the shell and its overpressure protection requirements.
- The Energy Institute *Guidelines* require updating to account for the mechanical response of the shell wall to ensure that heat exchangers and their overpressure protection systems are adequately designed to prevent a loss of containment in the unlikely but credible event of a tube rupture.

Acknowledgements

This work was conducted under the Energy Institute's Good Practice (Technical) Work Programme and funded by its Technical Partners, with co-funding provided by its Technical Company Members.

References

1. API Standard 521: *Pressure-relieving and Depressuring Systems*, seventh edition.
2. Energy Institute, 2015, *Guidelines for the safe design and operation of shell and tube heat exchangers to withstand the impact of tube failure*, second edition.

Notation

a	speed of sound in vapour, m s^{-1}
A	cross-sectional area, m^2
c	wavespeed through the liquid, m s^{-1}
C_D	coefficient of discharge of tube open end, -
DLF	dynamic load factor, -
E	Young's Modulus
f_s	breathing mode frequency of shell, Hz
P_{is}	pressure in liquid after initial surge, Pa
P_r	initial pressure of liquid in shell, Pa
P_0	initial pressure of gas in tubes, Pa

$p(t)$	pressure at any time (t), s
ΔP_{is}	initial surge pressure rise, Pa
q	ratio of the surge pressure divided by the initial pressure
r	mean radius, m
Δr	radial displacement, m
t	time, s
Δt_{min}	minimum rise time, s

Greek symbols

γ	ratio of specific heats, -
ρ	density of shell material, kg m^{-3}
ρ_l	density of liquid, kg m^{-3}
v	Poisson's Ratio
ω	natural frequency of vibration, Hz

Subscripts

s	shell
t	tube